Novel composite proton-exchange membrane based on proton-conductive glass powders and sulfonated poly (ether ether ketone)

Zhigang Di [b], Qiang Xie [a], Haibin Li [a, *], Dali Mao [b], Ming Li [b], Daowu Zhou [a], Lu Li [c]

[a] Institute of Fuel Cell, School of Mechanical Engineering, Shanghai Jiao Tong University, 800 Dong Chuan Road, Shanghai 200240, China
[b] School of Materials Science and Engineering, Shanghai Jiao Tong University, 800 Dong Chuan Road, Shanghai 200240, China
[c] Zhoushan Top-Membrane New Material Technology Co., Ltd, 2123 West Donghai Road, Zhoushan, China

HIGHLIGHTS

- The SiO_2−Nafion/sulfonated poly (ether ether ketone) (SPEEK) composite membranes are fabricated.
- The poor miscibility of Nafion with SPEEK is solved by fixing Nafion into the SiO_2 glass powder.
- A maximum of the proton conductivity of 0.018 S cm^{-1} is obtained from the composite membrane.
- A single fuel cell equipped with the composite membrane exhibits a peak power density of 589.2 mW cm^{-2}.

ARTICLE INFO

ABSTRACT

The SiO_2−Nafion/sulfonated poly (ether ether ketone) (SPEEK) composite membranes are fabricated by using the simple mechanical ball-milling process to combine SiO_2 glass powders with small portion of Nafion, in which SiO_2 glass powders are prepared by modified sol−gel progress and Nafion is embedded in situ into a highly porous silica network. The morphology, thermal and mechanical properties, pore structure, proton conductivity and fuel cell performance of the SiO_2−Nafion/SPEEK composite membranes are investigated. The poor miscibility of Nafion and sulfonated aromatic polymer is solved by fixing Nafion into SiO_2 glass powders. The composite membranes perform well even if the proportion of inorganic component in membranes is as high as 40 wt.%. A maximum of proton conductivity, 0.018 S cm^{-1}, is obtained from the membrane of 4(8Si−2N)/6SPEEK at 80 °C and 90% relative humidity, which is owing to its enhanced hygroscopicity and highly dispersed Nafion clusters. In addition, a single fuel cell equipped with the composite membrane shows a peak power density of 589.2 mW cm^{-2} at 70 °C.

1. Introduction

Proton-exchange membrane fuel cells (PEMFCs) are regarded as one of the most promising new energy devices for addressing energy and environmental issues because of their diverse advantages like low operating temperature, high efficiency and environmental friendliness. Proton-exchange membranes (PEMs) are one of the key components in PEMFCs. Among all kinds of proton exchange membranes, perfluorosulfonic acid (PFSA) type membranes such as Nafion® made by DuPont™ have been used extensively in current low-temperature PEMFCs owing to their high proton conductivity and good chemical stability. However, the application of this kind of membrane in fuel cells is restricted by their noticeable disadvantages such as high cost, high fuel permeability and loss of proton conductivity above 80 °C. Accordingly, it's strongly worthwhile to develop an alternative and cost-effective PEMs to promote a wider use of PEMFCs in stationary and vehicular applications.

The feasibility of hydrocarbon-based membranes as a substitute for Nafion has been explored by many researchers in the past few years [1–8]. Of all kinds of hydrocarbon-based membranes, the most studied one is the membrane based on aromatic poly (ether ether ketone) (PEEK), which is a thermally stable polymer with an aromatic, non-fluorinated backbone in which 1,4-disubstituted phenyl groups are separated by ether (−O−) and carbonyl (−CO−) linkages. Compared with PEEK, Sulfonated PEEK (SPEEK) possesses better mechanical properties, thermal stability and higher conductivity, all of which depend on the degree of sulfonation (DS) that can be controlled by changing the reaction time and temperature [5–9].

In addition, inorganic materials have also been widely studied that are used as non-proton-conductive additives or as proton

conductors in PEMs. Hygroscopic inorganic oxides, such as SiO_2, ZrO_2, and TiO_2, have been incorporated into organic PEMs to increase water retention under low humidity. Among these oxides, SiO_2 is the most important because of its low cost and easy synthesis. When used in a PEM, SiO_2 is usually prepared in situ from alkoxide tetraethylorthosilicate (TEOS) via sol–gel process [10]. The sol–gel-prepared SiO_2 powders have three-dimensional structure and are realistically denoted as $SiO_{2(1-x/4)}(OH)_x$, where x is greater than zero in order to achieve the porous and hygroscopic property desired. Generally, a maximum of ~10 wt.% of oxide can be added to a polymer matrix without reducing proton conductivity. Additionally, all of these oxides can be sulfonated, which makes them acidic and improves their proton conductivity. However, sulfonation is very complicated and doesn't necessarily boost its conductivity significantly and fuel-cell performance [11]. Several inorganic proton conductors can reach high proton conductivities of $10^{-2}-10^{-1}$ S cm^{-1} under certain conditions, which is comparable to that of Nafion® under proper and favorable conditions. These proton conductors include CsH_2PO_4 at 245 °C and 30% RH [12], $Zr(HPO_4)_2$ at 80 °C and 100% RH [13] as well as $P_2O_5-TiO_2$ at 80 °C and 100% RH [14]. Nevertheless, the power densities of fuel cells using inorganic proton-conductive membranes as electrolytes are much lower than those of fuel cells based on Nafion® membrane. For example, using phosphotungstic acid (HPW) $-P_2O_5-SiO_2$ membranes in fuel cells, Nogami et al. obtained a peak power density of 42 mW cm^{-2} in H_2/O_2 at ~30 °C and 30% RH [15]. Lu et al. obtained a peak power density of 95 mW cm^{-2} at 100 °C from the fuel cell using a phosphotungstic acid ($H_3PW_{12}O_{40}$)/mesoporous silica (MCM-41) membrane [16]. Ioroi et al. obtained a peak power density of 45 mW cm^{-2} from the fuel cell using the surface-modified porous glass with SO_3H attached on the surface of the pores [17]. Our group has prepared phosphosilicate ($SiO_2-P_2O_5$) glass membranes with high proton conductivity of 10^{-1} S cm^{-1} and assembled a fuel cell using that membrane, obtaining a peak power output of 207 mW cm^{-2} [18]. Despite the favorable properties of inorganic membranes such as low cost and high proton conductivity, their widespread applications are seriously hindered by their low power density mainly caused by their inflexibility and brittleness; and these unfavorable properties make the traditional membrane-electrode assembly (MEA) process using hot pressing unable to maximize the interface contact between the electrolyte and electrode [18].

Given their respective merits and demerits of organic and inorganic membranes, it's of great worth to prepare and explore the organic–inorganic hybrid membranes by incorporating inorganic phases into polymer matrix, which probably provides an efficient way to address the challenges faced by organic or inorganic membranes. In this study, $SiO_2-Nafion$ glass powders were prepared via sol–gel process and a low-temperature (150 °C) humid-annealing treatment. Large proportion of the powder was incorporated into a hydrophilic hydrocarbon-based SPEEK matrix by using mechanical ball-milling in order to form a $SiO_2-Nafion/$ SPEEK composite membrane. The composite membrane exhibits high proton conductivity, sufficient mechanical strength and flexibility. The peak power density of a single fuel cell equipped with the composite membrane reaches 589.2 mW cm^{-2} at 70 °C.

2. Experimental procedure

2.1. Materials

$Si(OC_2H_5)_4$ (TEOS, Sinopharm) and Nafion® dispersion (DUPONT DE1020 NAFION® Solution, 10 wt.% Nafion with terms of small aggregates in a mixture of low aliphatic alcohols and water, Ion Power. Inc) were used without further purification. Poly (ether ether

ketone) (PEEK) (Grade 450-P, Victrex Inc.) was dried under vacuum condition lower than 10^3 Pa at 110 °C for 24 h in a vacuum box before use.

2.2. Preparation of $SiO_2-Nafion/SPEEK$ composite membrane

The $SiO_2-Nafion$ glass was prepared via sol–gel method. First, TEOS, deionized water and hydrochloric acid were mixed in a molar ratio of 1: 4: 4×10^{-3} (TEOS: H_2O: HCl) and stirred for 1 h at room temperature. Different amounts of Nafion were added to the sol mixtures and then stirred for another 1 h until became transparent. The solutions thus obtained were transferred to polytetrafluoroethylene (PTFE) containers and kept at room temperature until gelation finished. Later, the obtained xerogels were treated by humid-annealing at 150 °C for 24 h under saturated water vapor. The $SiO_2-Nafion$ glass sheets after these treatments were crushed into micron-sized powders by an electric crusher and then the glass powder were screened by using an 800 mesh sieve. The resultant composite $SiO_2-Nafion$ glasses are designated as 9Si–1N, 8Si–2N and 7Si–3N, respectively, to indicate the different weight ratios of SiO_2 and Nafion in the glasses, namely, 9:1, 8:2 and 7:3.

The sulfonation of PEEK followed the method described previously [19]. PEEK powder (20 g) was slowly added to the pre-heated concentrated sulfuric acid (400 mL) and vigorously stirred for 2.5 h at 50 °C at the same time. The sulfonated polymer solution was then quickly poured into to a large ice-water bath to terminate the reaction; and the fibrous SPEEK polymer was precipitated from water. The collected polymer was washed repeatedly with deionized water until the value of pH became neutral and then dried overnight under vacuum condition lower than 10^3 Pa at 80 °C before use.

The inorganic-organic composite membranes were prepared by using mechanical ball-milling and solvent casting. Specifically, SPEEK was first dissolved in dimethylacetamide (DMAc) which was used as the solvent; and then different amounts of $SiO_2-Nafion$ glass powder with different Si/N ratios were added to it, respectively. The resultant mixtures were milled by using a planetary ball-mill apparatus (QM-3SP2, NanDa Instrument Plant) for 36 h at 450 r min^{-1}. The slurries obtained after being milled were cast onto glass plates using a doctor blade and then dried at 90 °C for 3 h under vacuum condition to form $SiO_2-Nafion/SPEEK$ composite membranes. The composite membranes were detached from the glass plates and stored in vacuum-sealed bags. The membranes were designated as $x(aSi-bN)/ySPEEK$, where x and y were the weight ratio of $SiO_2-Nafion$ glass powder and SPEEK, and a and b denoted the weight ratio of SiO_2 and Nafion in the $SiO_2-Nafion$ glass. The names and compositions of all membranes in this study are listed in Table 1.

2.3. Characterization

The infrared spectra of membranes were recorded on a Fourier transform infrared (FTIR) spectrometer (Nicolet 6700, Thermo Fisher Scientific Inc.). The porous structure of each membrane was analyzed via the nitrogen adsorption–desorption apparatus (TriStar II 3020, Micromeritics Inc.) after degassing under N_2 flow at 120 °C for 6 h. Scanning electron microscopy (SEM) images were obtained from an ultra-high-resolution field-emission SEM (S-4800, Hitachi Co.) using electron-beam deceleration mode. The method of liquid nitrogen brittle fracture was used to acquire the cross-sections of membranes; and Pt was sputtered on the cross-sections. Trace elemental analysis was conducted by an EDAX GENESIS XM2 energy dispersive X-ray spectrometer (EDS).

The mechanical properties of composite membranes were assessed on a dynamic mechanical analyzer (DMA 8000,

Table 1
Membranes names and their corresponding components.

Membrane name	Feed ratio of S:N in SiO$_2$–Nafion powders (weight ratio)	Ratio of SiO$_2$–Nafion powder:SPEEK in the composite membranes (weight ratio)
9Si–1N	9:1	/
4(9Si–1N)/6SPEEK	9:1	4:6
8Si–2N	8:2	/
4(8Si–2N)/6SPEEK	8:2	4:6
7Si–3N	7:3	/
4(7Si–3N)/6SPEEK	7:3	4:6

PerkinElmer) using a DMA-controlled force module with a stretching speed of 0.3 N min^{-1} at room temperature. Membranes, in a size of 30 mm long and 3 mm wide, were used for the test. The degradation of membranes were investigated by a thermal analyzer (SDT Q600, TA Instruments) over a temperature range of 40–780 °C at a heating rate of 15 °C min^{-1} under N$_2$ atmosphere.

Because proton transport occurs primarily in the through-plane direction in an operating fuel cell, the measurement of the through-plane conductivity is more important than the in-plane conductivity for evaluating membrane performance and predicting fuel cell performance [20]. Ma et al. reported that the proton conductivity values measured by using the 2- and 4-electrode methods in the direction of thickness fit very well, verifying the effectiveness of 2-probe method in measuring the conductivity of the through-plane direction [21,22]. Accordingly, 2-electrode method was adopted in this study. Proton conductivities were measured by an impedance/gain phase analyzer (SI 1260, Solartron) in a two-electrode geometry at an AC amplitude of 10 mV over a frequency range 10^{-1}–10^7 Hz. Before measured, the samples clamped between two Pt sheets were placed in an enclosed constant temperature and humidity chamber and kept for 2 h under each measurement temperature and humidity condition.

The proton conductivity, σ (S cm^{-1}), of membranes was calculated from the following formula:

$$\sigma = l/(AR) \tag{1}$$

where l is the thickness of the membrane, A is the area of the Pt sheet electrode in contact with the membrane and R is the membrane resistance determined from complex impedance plot [23].

The degree of sulfonation (DS) of SPEEK polymer was determined by titration with NaOH followed by back-titration with HCl. And ion exchange capacity (IEC) of SPEEK polymer was also measured by acid–base titration method. Specifically, for IEC test, the dried weighted membrane was immersed in a 2 M NaCl aqueous solution at 40 °C for 24 h under magnetic stirring. The H$^+$ ions, substituted by Na$^+$ ions, were released into the solution. The solution was then titrated at room temperature by a 0.025 M NaOH solution in which phenolphthalein was used as an indicator. The IEC of membrane was calculated from the following equation:

$$IEC = (C_{NaOH} \times V_{NaOH})/W_{dry} \tag{2}$$

where C_{NaOH} is the concentration of NaOH solution, V_{NaOH} is the volume of the NaOH solution consumed for titration and W_{dry} is the weight of the dried membrane.

To determine the water uptake and swelling ratio, the membranes were dried at 120 °C for 24 h and then their weights and lengths were measured. Thereafter, the membranes were immersed in distilled water at room temperature for 24 h until water uptake reached equilibrium. The weights and lengths of the wet membranes were recorded by using a micro-balance and a micrometer; and it's necessary to ensure that there is no residual water remaining on their surfaces before measurement. Water uptake was calculated from the following formula:

$$\text{Water uptake} = \left(W_{wet} - W_{dry}\right)/W_{dry} \times 100\% \tag{3}$$

where W_{wet} and W_{dry} are the weights of the wetted and dried membranes, respectively.

And the swelling ratio was calculated from the following formula:

$$\text{Swelling ratio} = \left(L_{wet} - L_{dry}\right)/L_{dry} \times 100\% \tag{4}$$

where L_{wet} and L_{dry} are the lengths of the wetted and dried membranes, respectively.

2.4. H$_2$/O$_2$ single fuel cell test

Gas-diffusion electrodes (GDEs) with Pt loading of 0.4 mg cm^{-2} (Hephas Energy Co. Ltd) were used to prepare a membrane electrode assembly (MEA) with an active area of 1 cm^2 (1 × 1 cm) by using hot-pressing method under the condition of 0.3 MPa and 135 °C for 90 s. The performance of the H$_2$/O$_2$ fuel cell assembled with the above-described MEA was evaluated by a fuel-cell tester (MiniTest3000, Toyo Corp.). The fuel cell was fuelled with hydrogen at the anode and oxygen at the cathode both at 1 atm. The gas flow rates of H$_2$ and O$_2$ were both set to 60 sccm. Cell performance was tested after the temperature reached 70 °C and the cell activation finished.

Electrochemical data, including polarization curves and electrochemical impedance spectroscopy (EIS) data, were collected by an impedance/gain-phase analyzer (SI1260, Solartron) and an electrochemical interface (SI1287, Solartron). The amplitude of the AC signal was 10 mV and the scanning frequency varied from 0.1 Hz to 1 MHz. The impedance spectra of the glass-membrane-based H$_2$/O$_2$ fuel cell were measured at 0.5 V. Additionally, we tested the fuel cell durability to characterize the overall performance of the composite-membrane-based MEA. The durability test was conducted by using a constant voltage output at 0.5 V; and the fuel cell operated continuously for more than 30 h before an unexpected anode fuel shutdown occurred.

3. Results and discussion

3.1. Fabrication and structure of the SiO$_2$–Nafion/SPEEK composite membranes

It has been reported that the surface area of PFSA is very low (typically 0.02 m^2 g^{-1} or less) because most of the active sites are buried within the polymer bulk. Thus, a channel constructed with sulfonic acid groups for proton transport reactions will have very low accessibility [24]. Given that Nafion is very expensive, we synthesized SiO$_2$–Nafion glass powders by using the sol–gel method in order to make full use of it. Nafion solution exists in terms of small aggregates suspended in the solvent. In the sol solution synthesized by the sol–gel process, there are mainly TEOS and Nafion suspension. The hydrophilic oligomers (Si(OC$_2$H$_5$)$_x$(OH)$_{4-x}$, x = 1-4) are generated by partial hydrolysis of TEOS [25] and aggregate around nanometer-sized colloidal dispersion of Nafion in a polar solvent. By the following gelation and humid treatment processes, the SiO$_2$–Nafion glass with Si–O–Si skeleton was obtained, in which Nafion clusters became entrapped within the SiO$_2$ network [26]. SPEEK with high DS and

many hydrophilic acid groups is known to have high conductivity; however, such SPEEK is more fragile and susceptible to swelling; and its long-term stability is considerably affected by the degradation induced by hydroxyl radicals. In contrast, a low DS endows SPEEK with low conductivity but high mechanical and thermal stability [27]. Many studies have shown that SPEEK with a DS of 50–80% seems to be an optimal compromise of adequate proton conductivity and modest stability [28]. The DS of the SPEEK prepared in this work is 0.67, which is determined by titration with NaOH followed by back-titration with HCl. The prepared SPEEK is used in this study to fabricate composite membrane. The chemical structure of SPEEK is shown schematically in Fig. 1, where X indicates the degree of sulfonation. According to the IEC test described previously, the ion exchange capacity of the SPEEK with a DS of 0.67 is 1.349 mmol g^{-1}.

In order to refine the SiO_2–Nafion glass powder and improve the uniformity of the mixtures, SiO_2–Nafion/SPEEK composite membranes were prepared by mechanically ball-milling the SiO_2–Nafion powders with various ratios of SiO_2 vs. Nafion and SPEEK. The composite membranes appeared yellowish-white and opaque. They were smooth and crack-free, indicating that mechanical ball-milling can effectively prepare composite membranes based on glass powder and polymer even if the proportion of glass powder is as high as 60 wt.%. For the composite membranes in this study, the weight ratio of glass powder to SPEEK is set as 4:6 in order to balance various properties, including conductivity, mechanical strength and flexibility.

Fig. 2 shows the SEM morphology of the glass powder of 8Si–2N and the cross-sectional image of 4(8Si–2N)/6SPEEK composite membrane as well as its EDS analysis. The comparison of SEM images in Fig. 2(a) and (b) shows that the SiO_2–Nafion particles in the membrane are formed by the aggregation of several to tens of nano-powder particles after the ball-milling of 36 h and that the size of the aggregated glass particles is ca. 100 nm, which is barely correlated with the size of the crushed SiO_2–Nafion glass powders. It implies that the particle size of SiO_2–Nafion glass powder in the composite membranes is mainly controlled by the duration of ball-milling process and thus the preparation of the membranes is reproducible.

EDS results in Fig. 2(c) and (d) show the contents of different elements of Point 1 and 2 in Fig. 2(a). The distinct difference in the EDS spectra between Fig. 2(c) and (d) is the presence or absence of Si-peak, which implies that Point 1 and 2 correspond to SiO_2–Nafion glass powder particle and the polymer matrix, respectively. In addition, EDS results also show that both Point 1 and 2 contain F and S elements and that Point 1 has higher F-peak while lower S-peak, compared to Point 2. This may be because part of the Nafion clusters exposed on the surface of the SiO_2–Nafion powder might have dissolved into the SPEEK solution during mechanical ball-milling, resulting in the presence of F component in SPEEK polymer matrix. Point 2 shows higher S-peak because SPEEK polymer matrix has a high content of sulfonic acid groups. Our research shows that the intertwining network of SPEEK molecular chains surrounded by the glass powder not only forms a strong backbone, which preserves the flexibility of the composite membrane, but also provides a continuous proton-conducting path

among the individual proton-conducting SiO_2–Nafion glass powder particles.

Phase separation in Nafion-SPEEK composite membranes was observed by Kim et al. that was caused by the poor miscibility of Nafion and sulfonated aromatic polymers [29]. Based on SEM and EDS of the composite membrane, we speculate that Nafion is mainly entrapped into the three-dimensional SiO_2 network as pore filler, which is compatible with our result that no phase separation of the polymers is observed. Both SPEEK and Nafion dispersing within the SiO_2 network provide a combined proton-conducting matrix; meanwhile, the glass particles mixed with Nafion provide efficient proton-conducting channels.

The porosity and accessibility of each SiO_2–Nafion glass powder was analyzed by nitrogen adsorption–desorption isotherms, and pore-size distributions were calculated by using the conventional Barrett–Joyner–Halenda (BJH) method. It is well known that the width of the hysteresis curve gives an indication of the accessibility of pores; and wider hysteresis means more interconnected pores [30]. As shown in Fig. 3(a), 8Si–2N glass powder displays a much larger hysteresis with an average pore volume of 0.141 mL g^{-1} compared to 9Si–1N (0.062 mL g^{-1}) and 7Si–3N (0.083 mL g^{-1}) glass powders. This is characteristic of mesoporous materials with capillary condensation, indicating that the degree of pore interconnection and corresponding gas accessibility is high. When SiO_2 powder is prepared via sol–gel process without a pore-forming agent, the gelation procedure and the subsequent thermal treatment will cause structural collapse and channel shrinkage. When the content of Nafion, acting as a filler, increases from 10 to 20 wt.% in the glass powders, the surface area and pore volume increase; however, when the Nafion content is up to 30 wt.%, the surface area and pore volume decrease. It may be because too much Nafion becomes entrapped in the SiO_2 network and thus blocked or wrapped the pores [31]. Fig. 3(b) shows that the glass powders have the similar peak pore sizes, with a diameter of 17.65 nm for 9Si–1N, 19.79 nm for 8Si–2N and 20.21 nm for 7Si–3N.

In Ref. [30], the pore structures of the PFSA/SiO_2 with various weight ratios of PFSA (Nafion resin) and TEOS were analyzed in details by N_2 adsorption–desorption. It has been reported that with the content of PFSA in PFSA/SiO_2 increasing, the surface area and pore volume will decrease gradually owing to the entrapping of PFSA in SiO_2 networks [30]. In our study, as shown in Fig. 3, the prepared SiO_2–Nafion glass powders are porous because it is difficult for the incorporated Nafion to fill pores thoroughly. The N_2 molecules could be adsorbed to the surfaces of the pore wall and Nafion cluster in the pores, which means that, for SiO_2–Nafion glass powders, the interconnected pores may lead to fuel leakage. On the other hand, however, the pore volumes and diameters of the SiO_2–Nafion/SPEEK composite membranes are not obtained by N_2 adsorption–desorption because their behavior is more like a nonporous solid. This implies that the SPEEK incorporated into the SiO_2–Nafion/SPEEK composite membranes probably blocks pores and that SPEEK content is also sufficient to block the fuel leakage.

Fig. 4 shows the FTIR spectra of the SiO_2–Nafion glass powders, the SiO_2–Nafion/SPEEK composite membranes and pure SPEEK. For the glass powders, the peaks at $\nu = 798$ may be assigned to the characteristic peaks of Si–O–Si bonds which were formed during
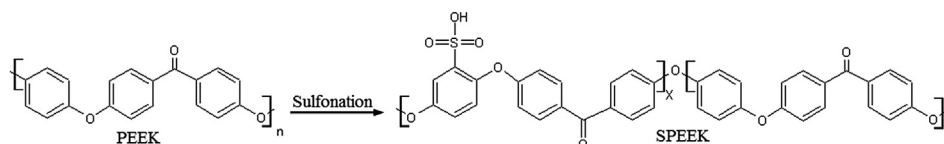

Fig. 1. Chemical structure of SPEEK produced by sulfonating PEEK. X and Y denote the sulfonated and unsulfonated portions, respectively.
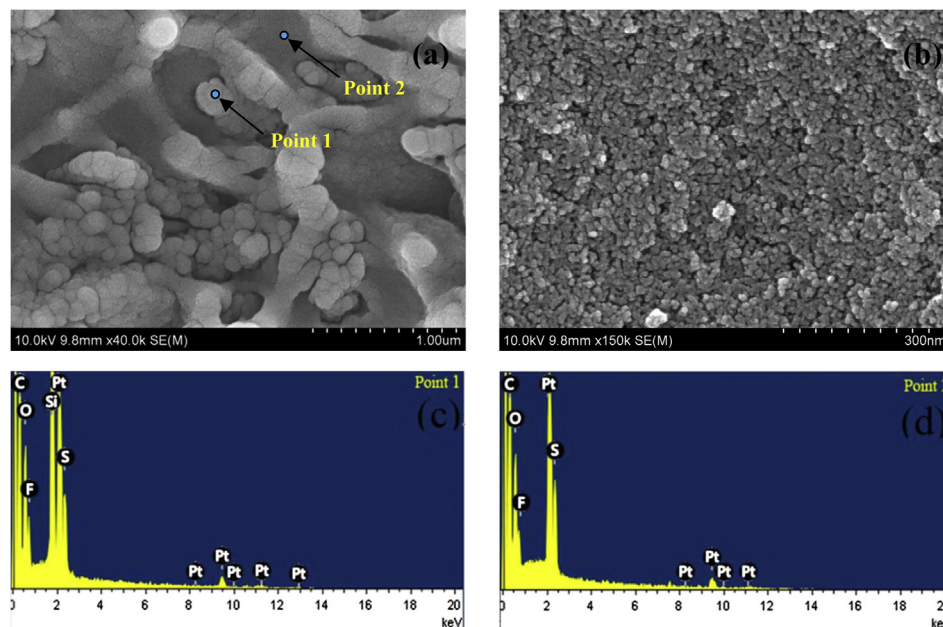
Fig. 2. (a) SEM cross-sectional image of the 4(8Si–2N)/6SPEEK composite membrane; (b) the SEM morphology of the glass powder of 8Si–2N; (c) and (d) EDS images of point 1 and 2 in (a).
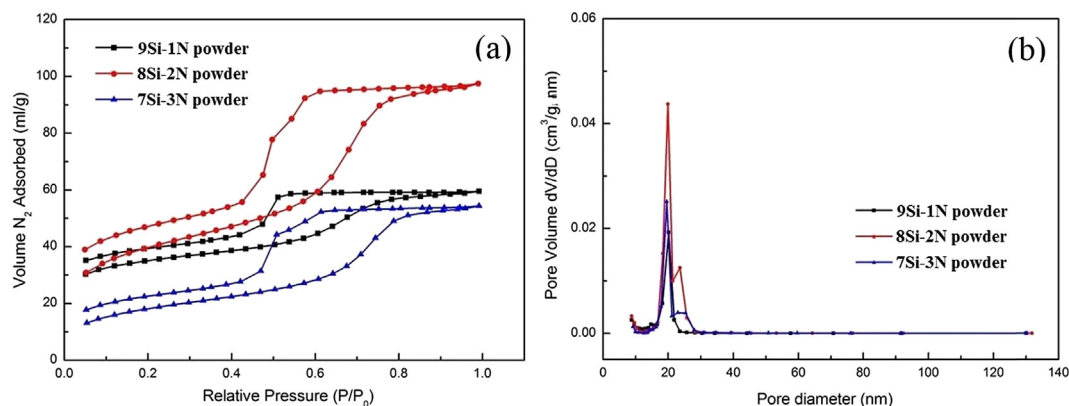

Fig. 3. (a) N_2 adsorption–desorption isotherms of SiO_2–Nafion glass powders; (b) pore-size distribution curves of SiO_2–Nafion glass powders.

the gelation and subsequent humid annealing treatment [32]. It provides evidence for the formation of the Si–O–Si skeleton during the condensation reaction. $v = 950$ cm^{-1} may be assigned to the Si–OH group [33]. In a typical sol–gel process, the hydrolysis reaction of TEOS is incomplete and various hydrophilic oligomers $(Si(OC_2H_5)_x(OH)_{4-x}, x = 0–4)$ are generated owing to partial hydrolysis [25]. In the humid-annealing process, water vapor is introduced, accelerating the hydrolysis of the rest of unhydrolyzed ethoxy groups. During the gelation and humid-annealing processes, the dehydration reaction occurs, resulting in the formation of a xerogel with a Si–O–Si network structure, in which a considerable amount of uncondensed Si–OH groups still exist.

Two peaks at $v = 1210$ and 1087 cm^{-1} are attributed to the C–F stretching modes of the perfluorosulfonic acid polymer (Nafion) [34]. For pure SPEEK and the SPEEK incorporated into the SiO_2–Nafion/SPEEK composites, the success of sulfonation was verified by the absorption peaks at $v = 1220$, 1072, and 1020 cm^{-1}, attributable to the O=S=O vibrations of the sulfonic acid group [35]. Peaks at $v = 1470$ and 1490 cm^{-1} may be attributed to C–C stretching modes of the newly sulfonated aromatic ring [19], and

the absorption at $v = 1645$ cm^{-1} corresponds to the carbonyl group of SPEEK [36].

3.2. Thermal and mechanical properties of the SiO_2–Nafion/SPEEK composite membranes

We used thermogravimetric analysis (TGA) under a nitrogen atmosphere to study the thermal degradation of the SiO_2–Nafion/SPEEK composite membranes and a pure SPEEK membrane. Fig. 5 shows the weight loss of each membrane versus temperature. For SPEEK, TGA curve features two main degradation stages corresponding to degradation of the sulfonic acid groups and thermal oxidation of the polymer main chain. The weight loss associated with both the dehydration of water molecules interacting with SO_3H or the SiOH groups through hydrogen bonds and the thermal degradation of sulfonic acid groups starts at 180 °C and reaches 30% at 350 °C [37]. The weight loss for temperatures above 500 °C may be attributable to thermal degradation of the main SPEEK chain, which reached 65% at 600 °C. The degradation of the SiO_2–Nafion/SPEEK composite membranes is significantly delayed compared
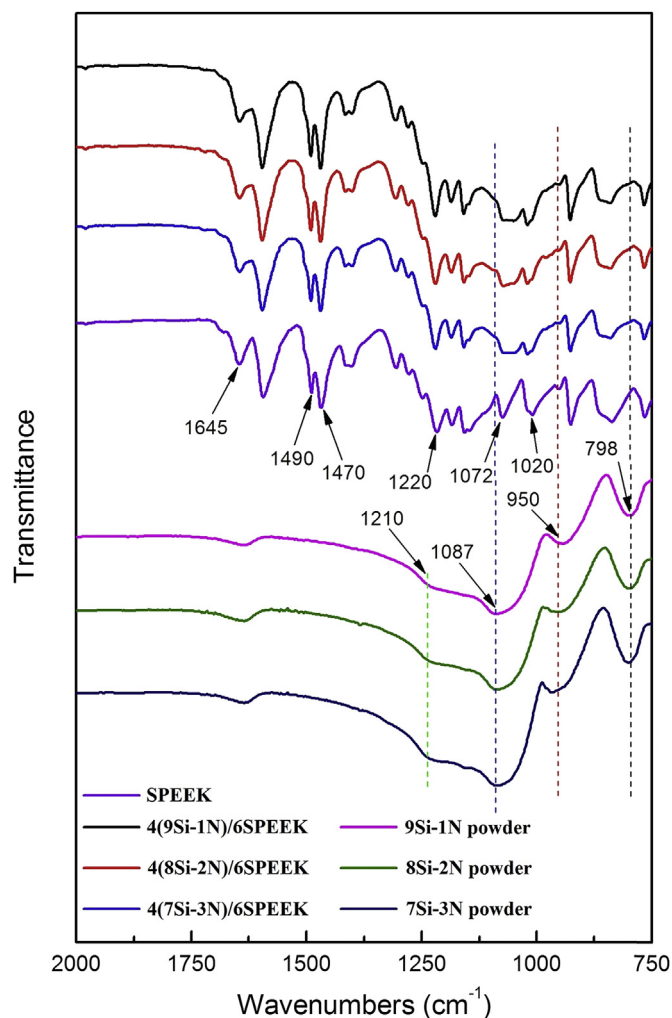
Fig. 4. Infrared spectra of SiO₂−Nafion glass powders, SiO₂−Nafion/SPEEK composite membranes and SPEEK polymer.

with that of pure SPEEK because of the incorporation of the glass powders. The ~7% weight loss before 300 °C may be credited to dehydration of absorbed water molecules involving in hydrogen bonds and the thermal degradation of sulfonic acid groups in both SPEEK and Nafion [38]. Degradation at 300−400 °C has been believed to originate from the decomposition of the perfluoroether side chains of Nafion [38]. The amount of residue after the elimination of organic components at high temperatures ($T > 700$ °C) agrees well with the portion of inorganic SiO_2 incorporated in each composite membrane. Note that the thermal degradation was studied under nitrogen atmosphere without oxygen; while a different weight loss may be obtained under oxygen atmosphere in a fuel cell.

Good mechanical strength is essential to PEMs for fuel-cell application. Fig. 6 shows the stress−strain behavior of the SiO₂−Nafion/SPEEK composite membranes at room temperature. All the composite membranes with 60 wt.% SPEEK have a tensile strength of ~23 MPa despite the disparity in the compositions of inorganic glass powders. This result suggests that the mechanical strength of membranes is mainly determined by the weight ratio between the SiO₂−Nafion glass powder and SPEEK. This tensile strength is much higher than that of a recast Nafion membrane, which is ~10 MPa [39]. Among the SiO₂−Nafion/SPEEK composite membranes, 4(7Si−3N)/6SPEEK membrane has the highest
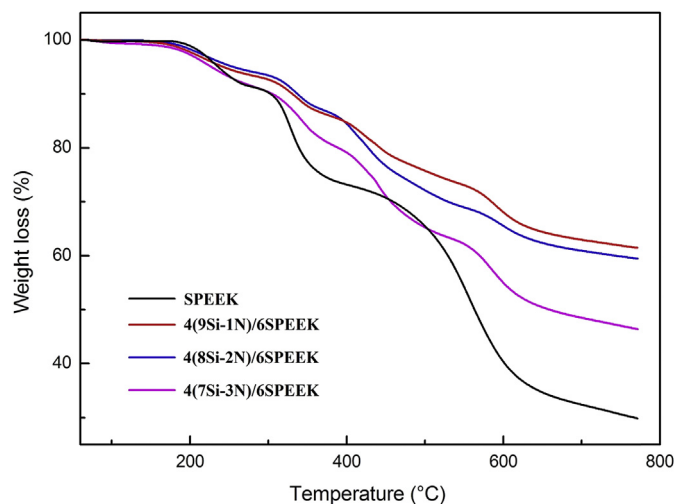

Fig. 5. TGA curves of SiO₂−Nafion/SPEEK composite membranes and pure SPEEK.

elongation, 1.8%, while the reason for this is not clear. Further study is definitely required.

3.3. Proton conductivity, water uptake and swelling ratios of the SiO₂−Nafion/SPEEK composite membranes

In this section we examined the proton conductivity of the composite membranes under various temperatures and relative humidity conditions. Fig. 7(a) shows the temperature dependence of the proton conductivity of pure SPEEK membrane, SiO₂−Nafion/SPEEK composites and recast Nafion membrane, which was measured at 90% RH. The conductivity of each membrane increased with temperature. The conductivities of the SiO₂−Nafion/SPEEK composite membranes are $10^{-3}-10^{-2}$ S cm^{-1}, much higher than that of the pure SPEEK membrane, which is because the SiO₂−Nafion glass powder not only acts as the water-absorption carrier but also as a powerful local proton-conducting medium in the SPEEK matrix. The 4(8Si−2N)/6SPEEK composite membrane exhibits the highest proton conductivity, 0.018 S cm^{-1} at 80 °C and 90% RH, slightly higher than that of recast Nafion membrane. Note that proton conductivity of 4(8Si−2N)/6SPEEK composite
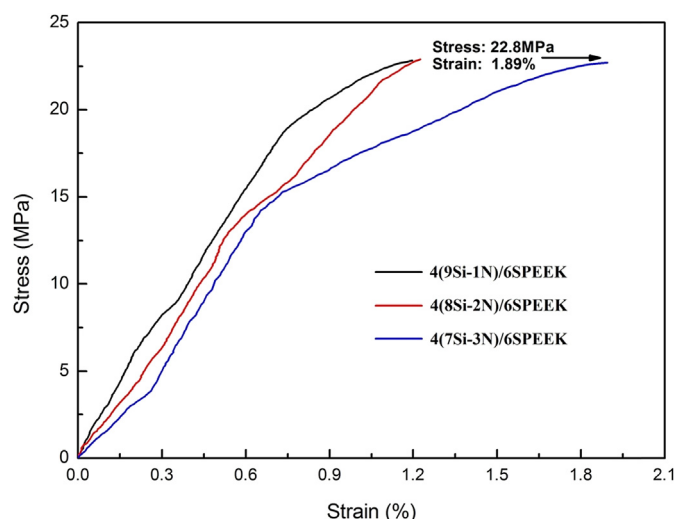

Fig. 6. Stress−strain curves of SiO₂−Nafion/SPEEK composite membranes.
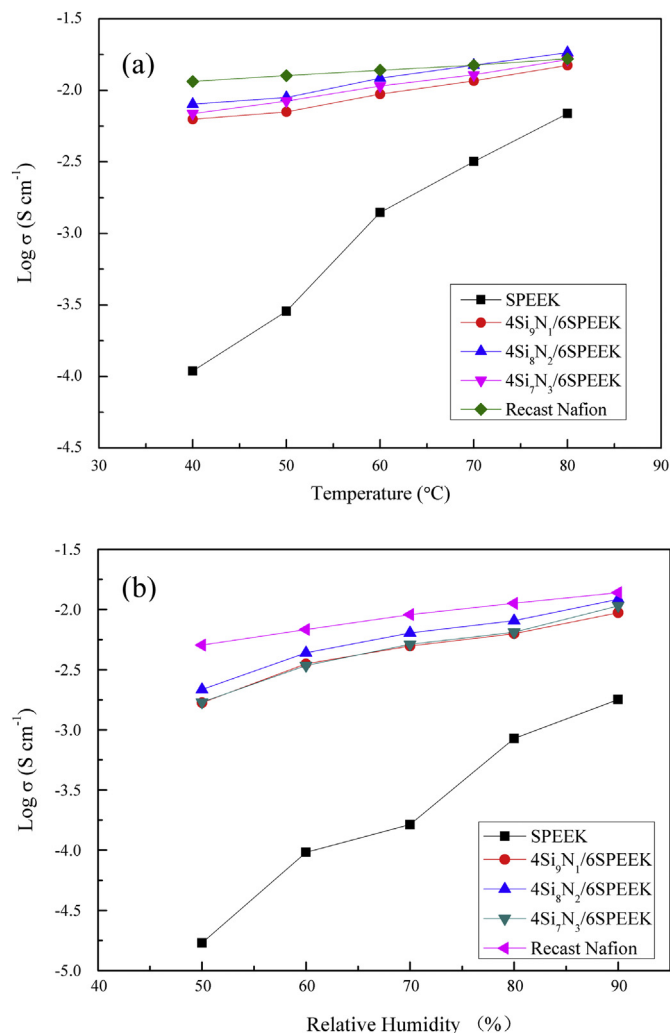
Fig. 7. (a) Temperature dependence of proton conductivity of pure SPEEK, SiO$_2$−Nafion/SPEEK composite membranes and recast Nafion membrane at 90% RH; (b) proton conductivity of pure SPEEK, SiO$_2$−Nafion/SPEEK composite membranes and recast Nafion membrane as a function of relative humidity at 60 °C.

membrane is higher than those of 4(9Si−1N)/6SPEEK and 4(7Si−3N)/6SPEEK composite membranes. This result just parallels that of the nitrogen adsorption−desorption isotherms test and might be attributed to the fact that the glass powder 8Si−2N has a proper pore structure and thus is able to maximize the Nafion content, increase the amount of proton conductor and maintain appropriate proton-transport channel simultaneously [31].

Fig. 7(b) shows the proton conductivity of pure SPEEK, SiO$_2$−Nafion/SPEEK composite membranes and recast Nafion membrane under various relative humidity conditions at 60 °C. As shown in Fig. 7(b), the conductivity of all membranes is sensitive to humidity and rises with the increase in relative humidity (RH) from 40 to 90%. It suggests that water molecules from ambient moisture could be absorbed into these membranes, thereby contributing to the migration of protons. And the conductivity of the composite membranes is much higher than that of pure SPEEK even if at low relative humidity conditions, which may be owing to the addition of Nafion. Specifically, Nafion itself is a fast proton conductor and could promote proton conduction of the composite membranes. As shown in Fig. 7(a) and (b), the recast Nafion membrane has high proton conductivity of ~10^{-2} S cm^{-1} all the time, much higher than that of the SPEEK polymer used in this study; and, in Fig. 7(b),

Nafion exhibits a quite satisfactory proton-conducting capability at low relative humidity conditions. Therefore, the incorporation of SiO$_2$−Nafion glass powders doped with Nafion could dramatically improve the proton conductivity of the composite membranes at low relative humidity conditions. Overall, proton conductivity experiment shows that by incorporating Nafion clusters into a highly porous silica glass network, the conductivity of the composite membranes can be elevated significantly even if a small proportion of Nafion.

The water uptake and swelling ratio are two important parameters of membranes for the investigation of PEMs. The 4(8Si−2N)/6SPEEK membrane has a water uptake of 22.4% and a very small swelling ratio of 1.1%, while the pure SPEEK membrane has a water uptake of 32.5% and a swelling ratio of 5.7%. Clearly, SiO$_2$−Nafion glass powders incorporated into the composite membrane plays a very important role in restraining the swelling of membrane body. The low-swelling property of the membrane may improve its mechanical durability and should be corresponding to a lower fuel leakage of fuel cell.

3.4. H$_2$/O$_2$ single fuel-cell testing

4(8Si−2N)/6SPEEK membrane with a thickness of ~72 μm was chosen to assemble a single fuel cell. For comparison, we also prepared fuel cells using pure SPEEK membrane and recast Nafion membrane with the similar thickness. After activating the fuel cells, we measured the polarization curves and impedance spectrum of each membrane, which are shown in Fig. 8(a) and (b), respectively. As shown in Fig. 8(a), the fuel cell based on 4(8Si−2N)/6SPEEK membrane has an open-circuit voltage of 0.992 V and a peak power density of 589.2 mW cm^{-2} while the fuel cell equipped with the pure SPEEK membrane has an open-circuit voltage of 0.914 V and a peak power density of 466.5 mW cm^{-2}. The peak power density of the fuel cell using recast Nafion is 632.7 mW cm^{-2}, slightly higher than that of the fuel cell using the 4(8Si−2N)/6SPEEK membrane. The output power of the fuel cell using the composite membrane was ~25% higher than that of the cell using pure SPEEK membrane, which is probably because the SiO$_2$−Nafion/SPEEK composite with incorporated SiO$_2$−Nafion glass powder has higher proton conductivity and less fuel leakage than pure SPEEK membrane.

Impedance analysis of the single fuel cell was carried out with a voltage load of 0.5 V; the impedance spectrum is shown in Fig. 8(b). The intercept in the high-frequency domain on the real axis represents the Ohmic resistance (R_Ω) of the fuel cell, which is 0.18 Ω cm^2 for the composite membrane and 0.26 Ω cm^2 for the pure SPEEK membrane. The difference of both resistances is primarily caused by the different proton conductivity of both membranes. The diameter of the semicircle in the low-frequency domain is the electrode resistance (R_e) from both the anode and cathode, which is 0.12 Ω cm^2 for the composite membrane and 0.11 Ω cm^2 for the pure SPEEK membrane; and this difference may be caused by the difference of the three-phase interface of the MEA at the cathode side even if GDEs and the operation conditions are the same for both test membranes [39]. Optimizing fuel-cell activation and adopting a catalyst-coated membrane (CCM) when MEA is assembled can further improve the power density of the fuel cell [18].

In order to assess the stability of 4(8Si−2N)/6SPEEK composite membrane operating in a fuel cell, we carried out a longevity experiment. Fig. 9 shows the stability of the output power with time elapsing under a cell voltage of 0.5 V. The assembly and operating conditions of the fuel cell for stability measurement are identical to those of the fuel cell in Fig. 8. Over the continuous measurement of 1800 min, the fuel cell shows remarkable stability at around 310 mW cm^{-2} with a 10 mW cm^{-2} fluctuation range. The
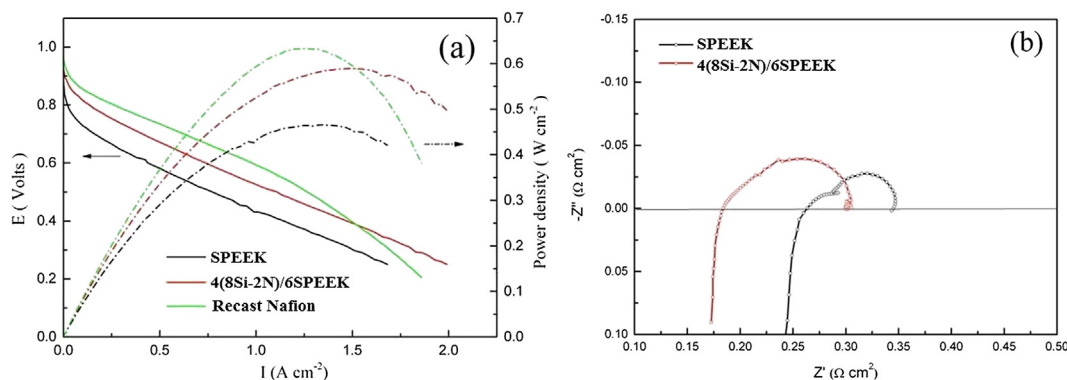
Fig. 8. (a) I–V and power density curves of SPEEK membrane, recast Nafion membrane and 4(8Si–2N)/6SPEEK composite membrane; (b) impedance spectrum of SPEEK-based and 4(8Si–2N)/6SPEEK -based fuel cells operating at 0.5 V.
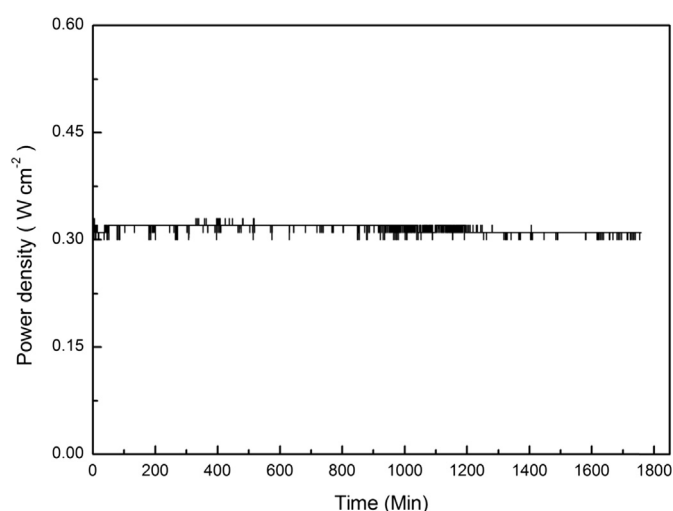

Fig. 9. Stability and durability test of the fuel cell equipped with 4(8Si–2N)/6SPEEK composite membrane at 0.5 V.

open circuit voltage (OCV) analysis of the fuel cell equipped with 4(8Si–2N)/6SPEEK composite membrane was also carried out for the membrane stability evaluation. The experiment lasted nearly 150 h under the same condition as the above constant voltage test.
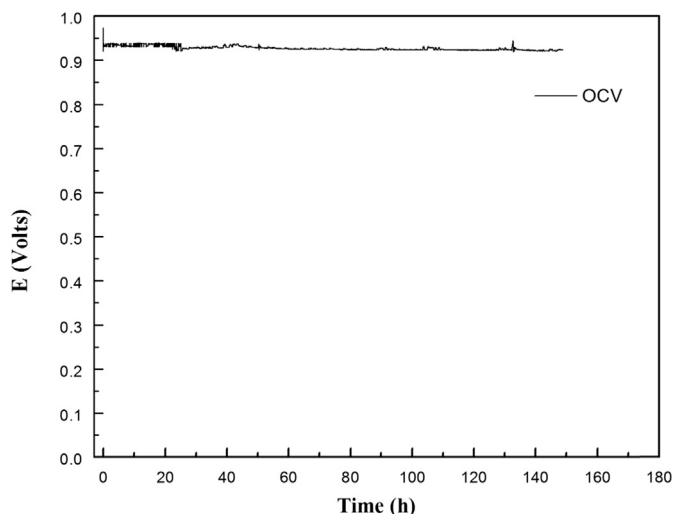

Fig. 10. Open circuit voltage test of the fuel cell equipped with 4(8Si–2N)/6SPEEK composite membrane.

Fig. 10 shows that the performance of the fuel cell with 4(8Si–2N)/6SPEEK composite membrane does not exhibit obvious drop in the OCV test. This result demonstrates the high stability of the SiO$_2$–Nafion/SPEEK composite membrane operating in a fuel cell. The evaluation of a longer running-time stability of the composite membrane is certainly required; and we are currently conducting these experiments in our laboratory.

4. Conclusion

SiO$_2$–Nafion glass powders were prepared by using sol–gel approach, in which a small amount of highly proton-conductive Nafion resin was incorporated into a highly porous silica network. Meanwhile, the SiO$_2$–Nafion/SPEEK composite membranes were fabricated by mixing the glass powders containing various ratios of SiO$_2$ and Nafion with SPEEK polymer via mechanical ball-milling. The obtained composite membranes exhibit good flexibility and high tensile strength even if the content of inorganics is up to 40 wt.%. And all the prepared composite membranes have higher proton conductivity than pure SPEEK under the same measurement conditions. Among these composite membranes, 4(8Si–2N)/6SPEEK composite membrane has a maximum proton conductivity of 0.018 S cm^{-1} at 80 °C and 90% RH. In addition, a single H$_2$/O$_2$ fuel cell equipped with this composite membrane shows a peak power density of 589.2 mW cm^{-2} at 70 °C. All these attractive performances of the composite membrane imply that this newly developed SiO$_2$–Nafion/SPEEK composite membrane is likely to become a promising alternative to pure perfluorosulfonic membranes for PEMFCs and Direct Methanol Fuel Cells (DMFCs).

References

[1] J.T. Wang, J.S. Wainright, R.F. Savinell, M. Litt, J. Appl. Electrochem. 26 (1996) 751–756.
[2] H. Ben Youcef, S.A. Guersel, A. Buisson, L. Gubler, A. Wokaun, G.G. Scherer, Fuel Cells 10 (2010) 401.
[3] C. Manea, M. Mulder, J. Membr. Sci. 206 (2002) 443–453.
[4] J. Rozière, D.J. Jones, Annu. Rev. Mater. Res. 33 (2003) 503–555.
[5] T.J. Peckham, S. Holdcroft, Fuel Cells 22 (2010) 4667–4690.
[6] M. Gil, X.L. Ji, X.F. Li, H. Na, J.E. Hampsey, Y.F. Lu, J. Membr. Sci. 234 (2004) 75–81.
[7] F. Trotta, E. Drioli, G. Morggalio, E.B. Poma, J. Appl. Polym. Sci. 70 (1998) 477.

[8] S.P. Jiang, Z.C. Liu, Z.Q. Tian, Adv. Mater. 18 (2006) 1068–1072.
[9] A.F. Ismail, N.H. Othma, A. Mustafa, J. Membr. Sci. 329 (2009) 18–29.
[10] N.H. Jalani, K. Dunn, R. Datta, Electrochim. Acta 51 (2005) 553–560.
[11] F. Lónyi, J. Valyon, J. Engelhardt, F. Mizukami, J. Catal. 160 (1996) 279–289.
[12] D.A. Boysen, T. Uda, C.R.I. Chisholm, S.M. Haile, Science 68 (2004) 303.
[13] C. Yang, S. Srinivasan, A.B. Bocarsly, S. Tulyani, J.B. Benziger, J. Membr. Sci. 237 (2004) 145–161.
[14] S.P. Tung, B.J. Hwang, J. Mater. Chem. 15 (2005) 3532–3538.
[15] T. Uma, M. Nogami, Chem. Mater. 19 (2007) 3604–3610.
[16] S.F. Lu, D.L. Wang, S.P. Jiang, Y. Xiang, J.L. Lu, J. Zeng, Adv. Mater. 22 (2010) 971.
[17] T. Ioroi, K. Kuraokaa, K. Yasuda, Electrochem. Solid State Lett. 7 (2004) 394.
[18] Z. Di, H. Li, M. Li, D. Mao, X. Chen, M. Xiao, J. Gu, J. Power Sources 207 (2012) 86–90.
[19] P.X. Xing, G.P. Robertson, M.D. Guiver, S.D. Mikhailenko, K.P. Wang, S. Kaliaguine, J. Membr. Sci. 229 (2004) 95–106.
[20] K.R. Cooper, ECS Trans. 41 (1) (2011) 1371–1380.
[21] S.H. Ma, A. Kuse, Z. Siroma, K. Yasuda, Espec. Technol. Rep. 20 (2005) 12.
[22] S.H. Ma, H. Tanaka, Espec. Technol. Rep. 23 (2007) 1.
[23] H. Li, T. Kunitake, Microporous Mesoporous Mater. 97 (2006) 42–48.
[24] M.A. Harmer, W.E. Farneth, Q. Sun, J. Am. Chem. Soc. 118 (1996) 7708–7715.
[25] S.J. Huang, H.K. Lee, W.H. Kang, Bull. Korean Chem. Soc. 26 (2005) 241.
[26] M.A. Harmer, Q. Sun, A.J. Vega, W.E. Farneth, A. Heidekum, W.F. Hoelderich, Green Chem. 2 (2000) 7–14.
[27] F. Wang, J. Li, T. Chen, J. Xu, Polymer 40 (1999) 795–799.
[28] P. Judeinstein, C. Sanchez, J. Mater. Chem. 6 (4) (1996) 511–525.
[29] I.T. Kim, J. Choi, S.C. Kim, J. Membr. Sci. 300 (2007) 28–35.
[30] H.K. Yuan, X.H. Ma, Z.L. Xu, Sci. China Chem. 54 (2011) 257–262.
[31] P. Innocenzi, J. Non Cryst. Solids 316 (2003) 309–319.
[32] H.N. Lim, M.A. Yarmo, N.M. Huang, P.S. Khiew, W.S. Chiu, J. Phys. Sci. 20 (2) (2009) 23–36.
[33] Q. Deng, C.A. Wilkie, R.B. Moore, K.A. Mauritz, Polymer 39 (1998) 5961–5972.
[34] P. Krishnan, J.S. Park, C.S. Kim, J. Membr. Sci. 279 (2006) 220–229.
[35] N. Intaraprasit, P. Kongkachuichay, J. Taiwan Inst. Chem. Eng. 42 (2011) 190–195.
[36] H.K. Kim, H.T. Ju, J.W. Hong, Eur. Polym. J. 39 (2003) 2235–2241.
[37] V.D. Notoa, N. Boarettoa, E. Negroa, G.A. Giffin, S. Lavina, S. Polizzic, Int. J. Hydrogen Energy 37 (2012) 6199–6214.
[38] P. Krishnan, J.S. Park, T.H. Yang, W.Y. Lee, C.S. Kim, J. Power Sources 163 (2006) 2–8.
[39] X.Z. Yuan, C.J. Song, H.J. Wang, J.J. Zhang, Fuel Cells 5 (2010) 10.